This is a repository copy of *Glucose-bearing biodegradable poly(amino acid) and poly(amino acid)-poly(ester) conjugates for controlled payload release*.

White Rose Research Online URL for this paper:
http://eprints.whiterose.ac.uk/106537/

Version: Supplemental Material

Glucose-Bearing Biodegradable Poly(amino acid) and Poly(amino acid)-Poly(ester) Conjugates for Controlled Payload Release

Mthulisi Khuphe and Paul D. Thornton*

School of Chemistry, University of Leeds, Woodhouse Lane, Leeds, LS2 9JT
paul.d.thornton@leeds.ac.uk

Additional Analytical Methods

Fourier Transform Infrared Analysis

Polymers were dried *in vacuo* (50 °C) for 24 hours prior to infrared analysis. Spectra were then recorded on a Bruker ALPHA-P FTIR spectrometer equipped with Bruker OPUS 7.0 software and a diamond attenuated total reflectance (ATR) accessory, by accumulating 32 scans.

Dynamic Light Scattering (DLS)

Dynamic light scattering (DLS) analysis was performed on a Malvern Zetasizer Nano ZS series instrument equipped with a 4 mW He-Ne laser operating at a wavelength of 633 nm and an avalanche photodiode (APD) detector. The non-invasive back scatter optic arrangement was used to collect the light scattered, at an angle of 173 °C. Samples were equilibrated for 2 minutes and analysed at 37 °C in a disposable 12 mm polystyrene cuvette. Data was processed by cumulative analysis of the experimental correlation function and the diameter of the particles was computed from the diffusion coefficients using Stokes–Einstein's equation. Measurements were carried out in triplicate.

Transmission Electron Microscopy (TEM)

Nanoparticles were obtained using the dialysis method, as described in the main text. A pipette was used to deposit a drop from the nanoparticle sample onto a carbon-coated copper grid. The solvent was then allowed to dry completely prior to analysis. TEM measurements were subsequently performed on a Titan Themis G2300KV instrument from FEI Instruments, operated at an accelerating voltage of 80 kV.

Scanning Electron Microscopy (SEM)

A glass pipette was used to deposit a drop of the nanoparticle solution onto a glass slide suitable for microscopy observations and the drop was allowed to air-dry. The glass slide was then mounted onto an SEM stub by using conductive tape and the previously dried samples were sputter-coated with a thin layer of gold using a Quorum Q150RS sputter-coater. Coated samples were subsequently analysed for particles size and morphology by employing a JEOL JSM-6610LV microscope (Oxford Instruments) equipped with a field emission electron gun. The working distance was varied between 10 and 17 mm and accelerating voltage between 5 and 15 kV was applied.

Advanced Polymer Chromatography (APC)

Advanced Polymer Chromatography (APC) analyses (DMF eluent, 1 g/L LiBr) were carried out using an ACQUITY APC AQ (200Å, 2.5 µm) column packed with bridged ethylene hybrid particles, on a Waters ACQUITY APC system equipped with an ACQUITY refractive index (ACQ-RI) detector. Column temperature was maintained at 40 °C and the flow rate at 0.5 mL/minute. System calibration was done using poly(methyl methacrylate) standards and data was processed using Empower 3 software. Glu-poly(Sar)-*b*-poly(PheLA): APC (DMF eluent, 1 g/L LiBr; M_w 4449 Da, Mn 4221 Da, PDI 1.05); Glu-poly(Sar)-*b*-poly(Phe): APC (DMF eluent, 1 g/L LiBr; M_w 4466 Da, Mn 4234 Da, PDI 1.05).

Ultraviolet-Visible (UV-Vis) Spectrophotometry

Absorbance readings (190 - 750 nm) were performed on a dual beam Varian Cary 50 UV0902M112 UV-Vis spectrophotometer (Agilent Technologies) equipped with a xenon pulse

lamp and Varian Cary WinUV 3.0 software. Samples were analysed in UV micro quartz cuvettes (10 mm, 700 µL and 1700 µL, black wall).

Critical Aggregation Concentration (CAC) Studies

Glu-poly(Sar)-b-poly(PheLA) and Glu-poly(Sar)-b-poly(Phe) solutions with polymer concentrations ranging from 10^{-5} mg/mL to 1 mg/mL were prepared in HPLC-grade water (18.2 M.Ω), respectively. Subsequently, light scattering studies were performed polymer solutions using a Malvern ZetaSizer Nano Series ZS instrument equipped with a 4 mW He-Ne laser operated at a wavelength of 633 nm. The non-invasive back scatter optic arrangement was used to collect scattered light at an angle of 173 °C. Samples were analysed in disposable quartz cuvettes at 37 °C. The critical aggregation concentration was determined from monitoring the change in the intensity of the scattered light (kilo counts per second (kcps)) in response to the concentration of the polymer.

Preparation of Rhodamine B-Loaded Nanoparticles

The loading procedure was adapted from methods detailed by Xu *et.al* [1] and Cheng *et.al* [2]. The absorbances of supernatants obtained after encapsulation of rhodamine-B were measured at the λ_{max} (554 nm). Absorbance values recorded before and after rhodamine B-encapsulation were then used to estimate the concentration of rhodamine B that was encapsulated in the nanoparticles and the loading efficacy (Eqn. 1 and Table S1).

$$\% \text{ Encapsulation} = [\frac{(\text{Total Rh. B content before loading} - \text{Rh.B in supernatant after loading})}{\text{Total Rh.B content before loading}}] * 100 \quad \text{Eq....(1).}$$

Table S1. Encapsulation of rhodamine B in glyconanoparticles.

	Amount Encapsulated (µM)	Encapsulation Efficiency (%)
Glu-poly(Sar)-*b*-poly(PheLA)	16.8	49.3
Glu-poly(Sar)-*b*-poly(Phe)	16.7	49.1

Analyses of Cyclic Monomers
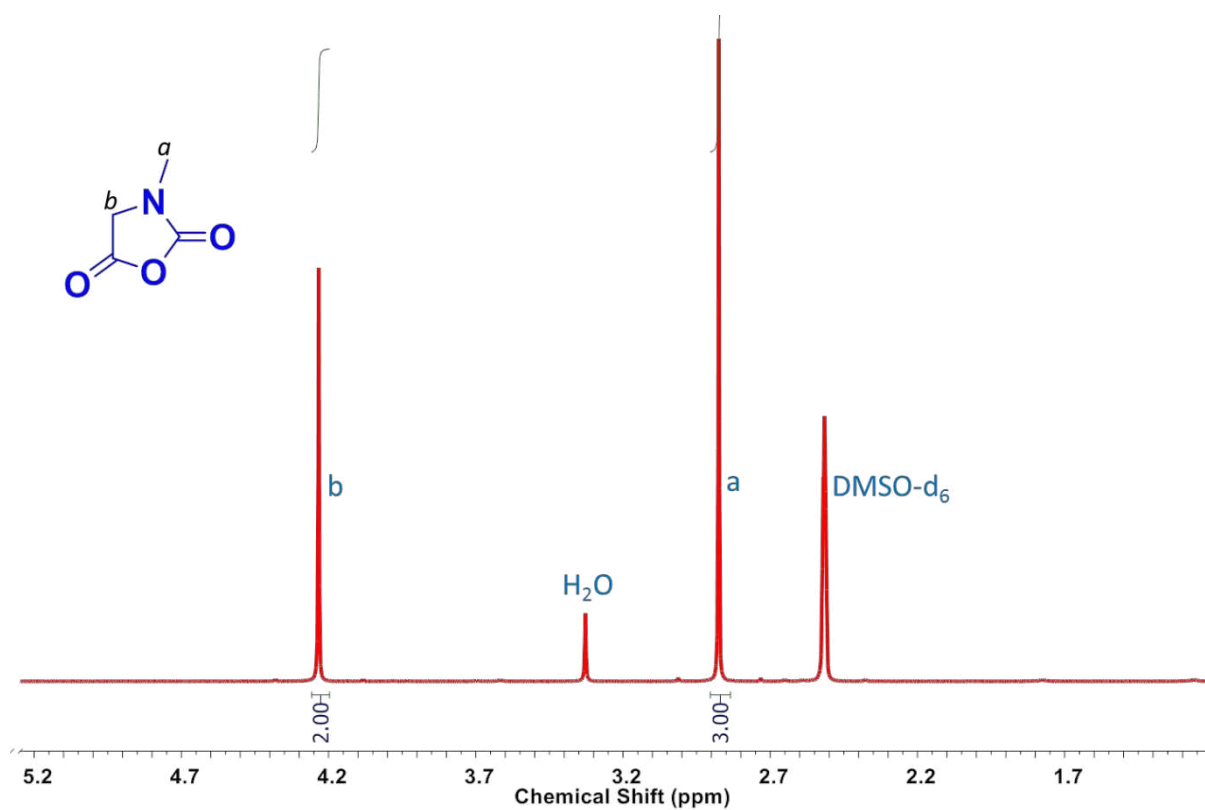

Figure S1. ^{1}H NMR spectrum of Sarcosine N-Carboxyanhydride in DMSO-d$_6$.
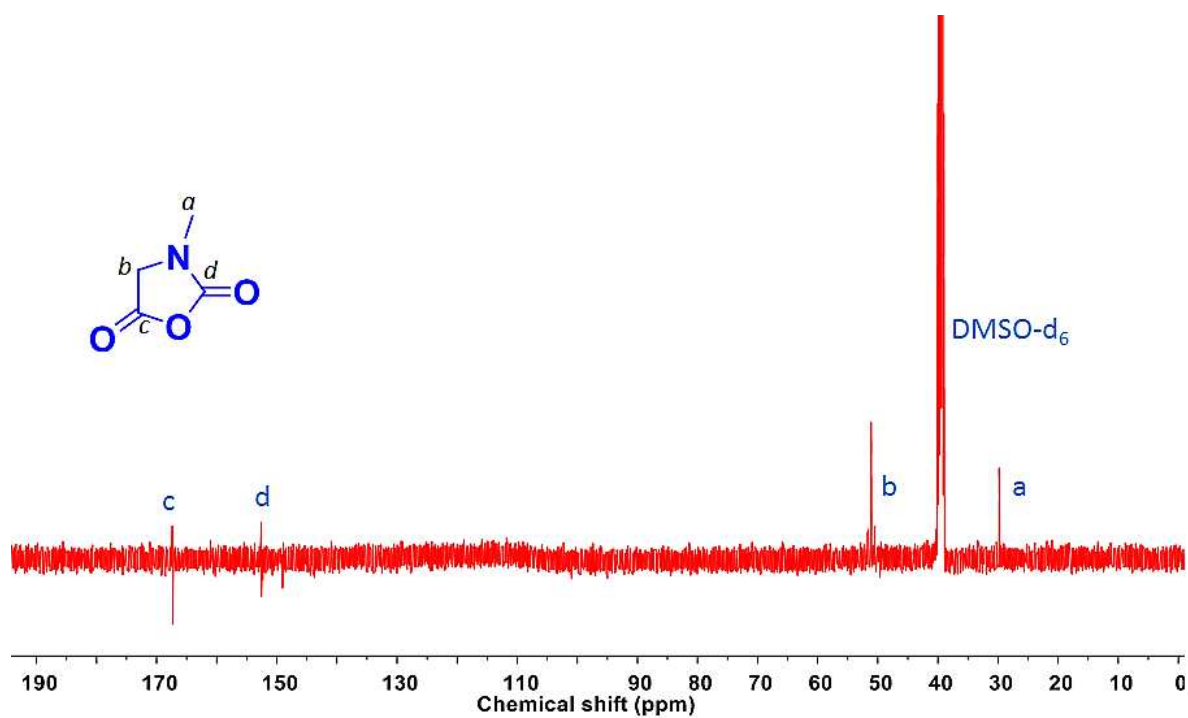
Figure S2. ^{13}C NMR spectrum of Sarcosine N-Carboxyanhydride in DMSO-d$_6$.

Table S2. Atomic composition of Sarcosine N-Carboxyanhydride

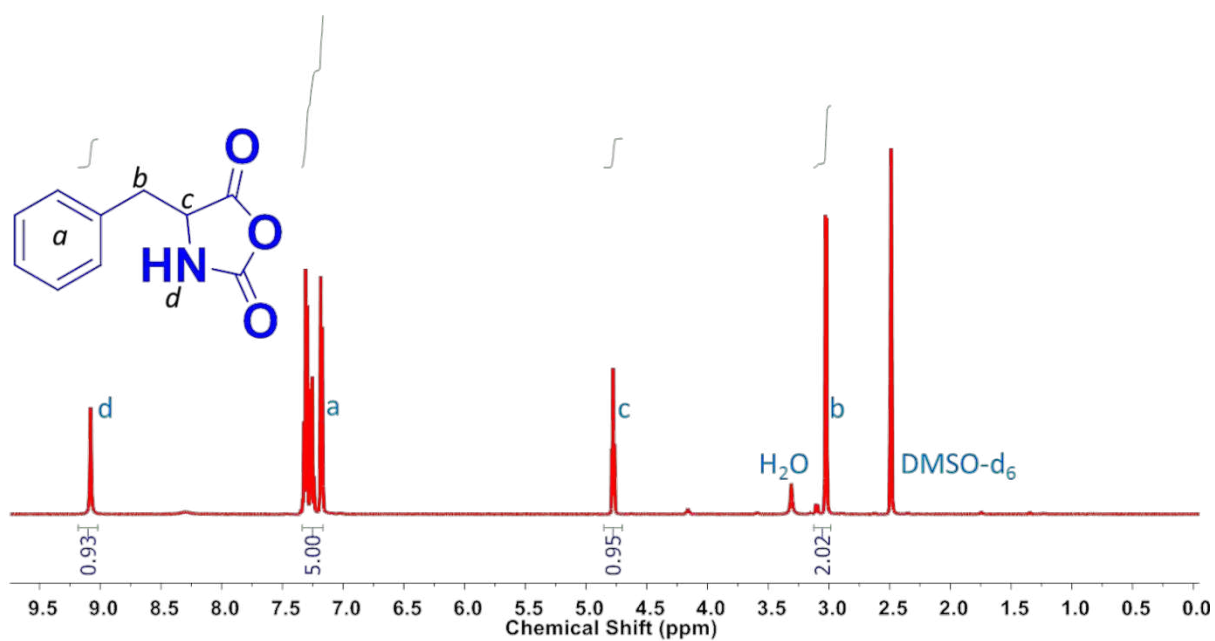|	% Carbon	% Nitrogen	% Hydrogen
Theoretical	41.75	12.17	4.38
Actual	41.69	12.22	4.41

Figure S3. ^{1}H NMR spectrum of L-Phenylalanine N-Carboxyanhydride in DMSO-d$_6$.

Table S3. Atomic composition of L-Phenylalanine N-Carboxyanhydride

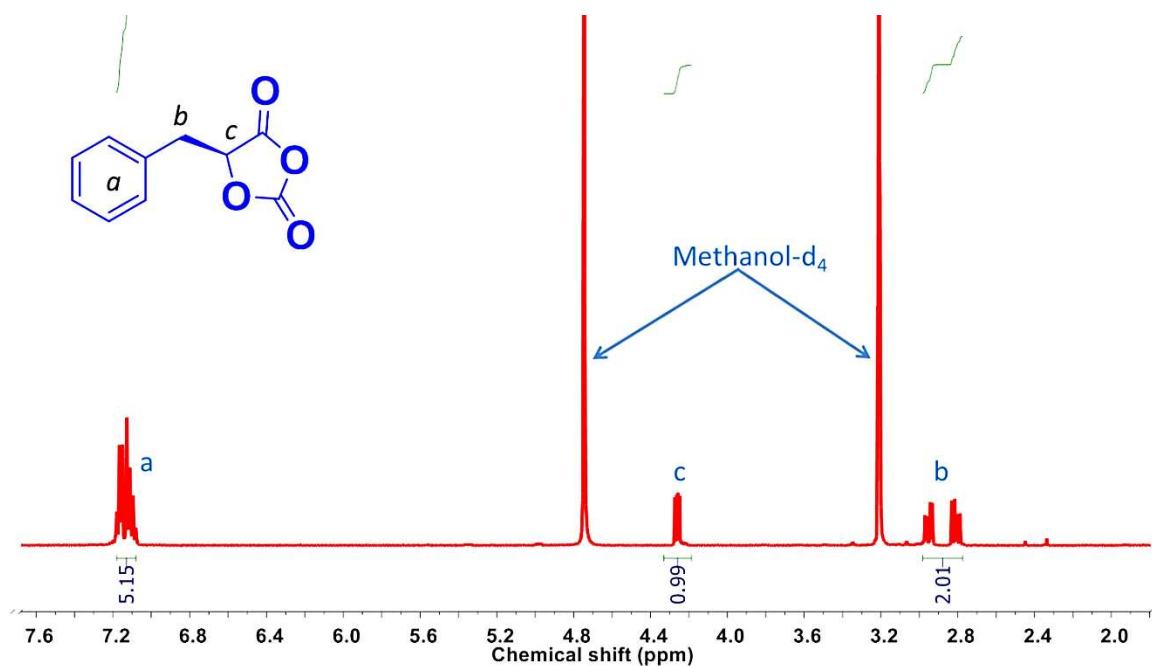|	% Carbon	% Nitrogen	% Hydrogen
Theoretical	62.82	7.33	4.75
Actual	62.79	7.35	4.77

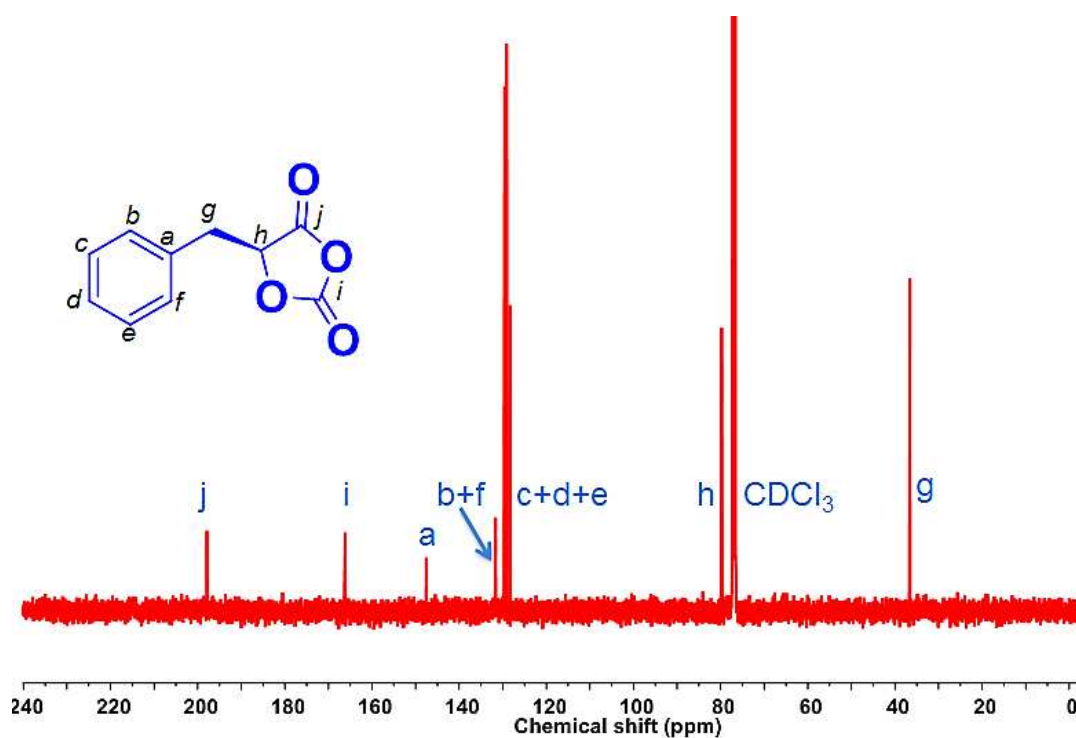Figure S4. ^{1}H NMR spectrum of L-Phenylalanine O-Carboxyanhydride in methanol-d$_4$.

Figure S5. ^{13}C NMR spectrum of L-Phenylalanine O-Carboxyanhydride in Chloroform-d.

Table S4. Atomic composition of L-Phenylalanine *O*-Carboxyanhydride

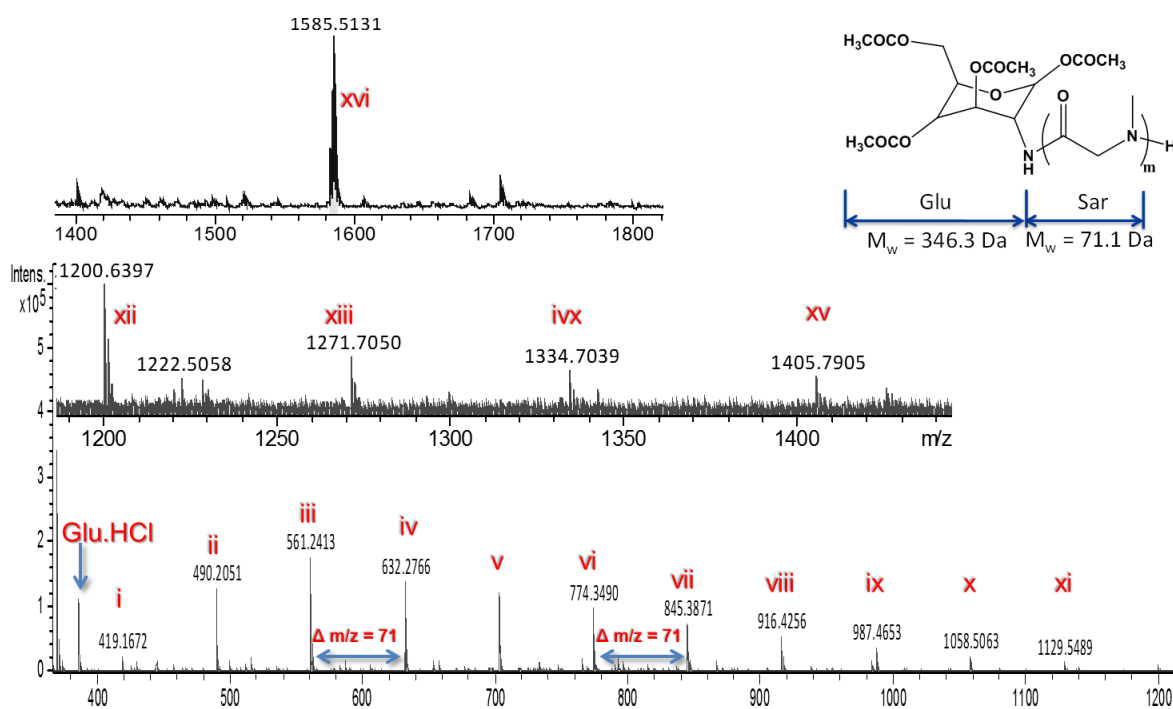|	% Carbon	% Hydrogen
Theoretical	62.50	4.20
Actual	62.52	4.21

Analyses of Polymers

Figure S6. ESI MS analysis of the reaction mixture in order to ascertain the feasibility of ROP of Sar NCA from a GluAm molecule confirmed the presence of Glu-(Sar) macromolecules. These have been assigned as; i: Glu-$(Sar)_1$, ii: Glu-$(Sar)_2$, iii: Glu-$(Sar)_3$, iv: Glu-$(Sar)_4$, v: Glu-$(Sar)_5$, vi: Glu-$(Sar)_6$, vii: Glu-$(Sar)_7$, viii: Glu-$(Sar)_8$, ix: Glu-$(Sar)_9$, x: Glu-$(Sar)_{10}$, xi: Glu-$(Sar)_{11}$, xii: Glu-$(Sar)_{12}$, xiii: Glu-$(Sar)_{13}$, ivx: Glu-$(Sar)_{14}$, xv: Glu-$(Sar)_{15}$, xvi: Glu-$(Sar)_{17}$.
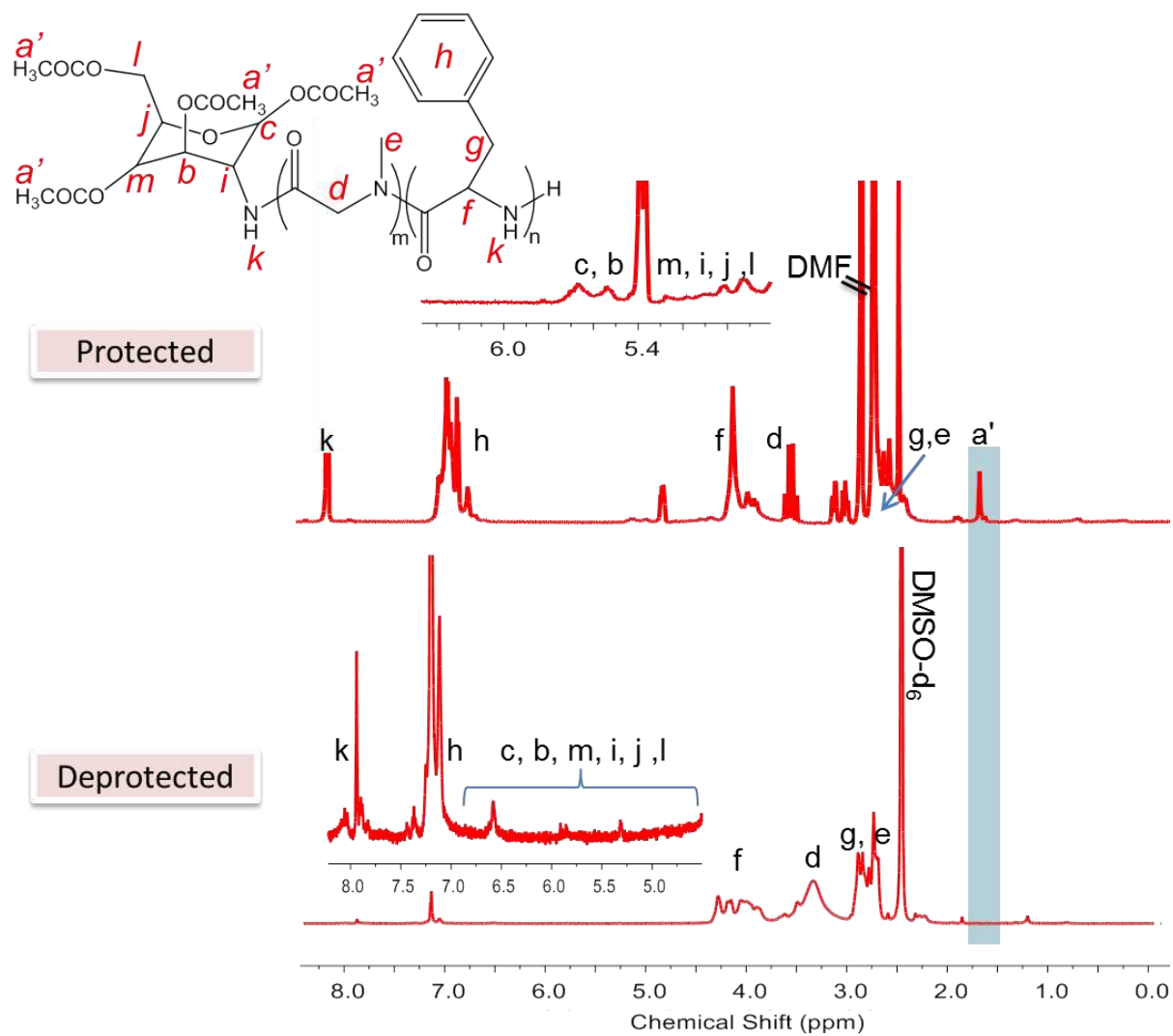
Figure S7. ^{1}H NMR spectra of Glu-poly(Sar)-b-poly(Phe) before and after removal of acetyl protecting groups from GluAm moieties.
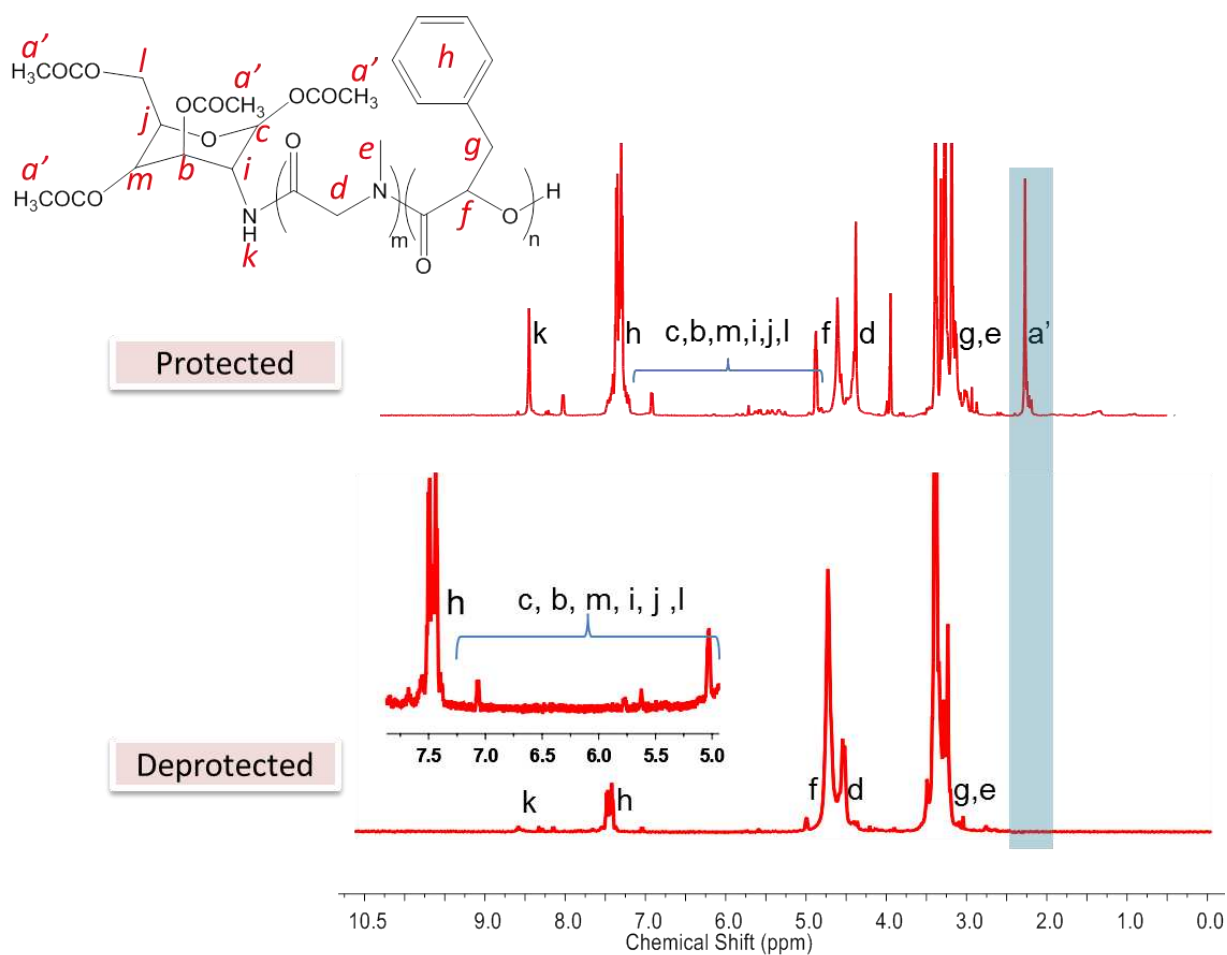
Figure S8. ^{1}H NMR spectra of Glu-poly(Sar)-*b*-poly(PheLA) before and after removal of acetyl protecting groups from GluAm moieties.

Fourier Transform Infrared Analyses

Figure S9. FTIR spectra of Glu-poly(Sar)-*b*-poly(PheLA) before (a) and after (b) cleaving off the acetyl protecting groups from the terminal sugar moieties. The emergence of the broad OH stretch (*ca* 3420 cm^{-1}) on the FTIR spectrum of the deprotected polymer (b) confirmed the removal of the acetyl groups.
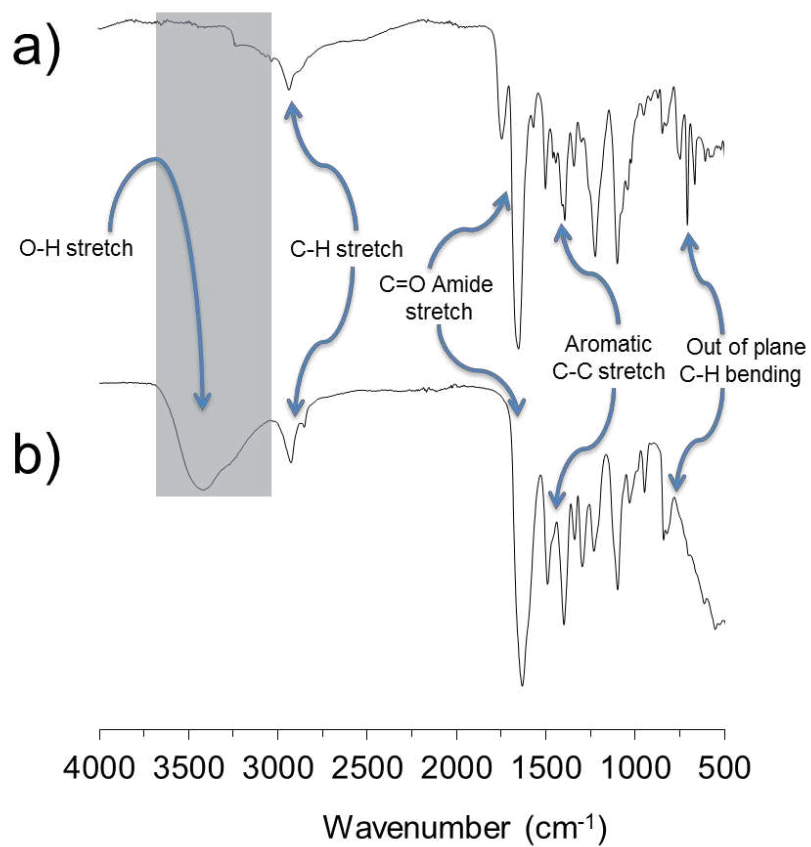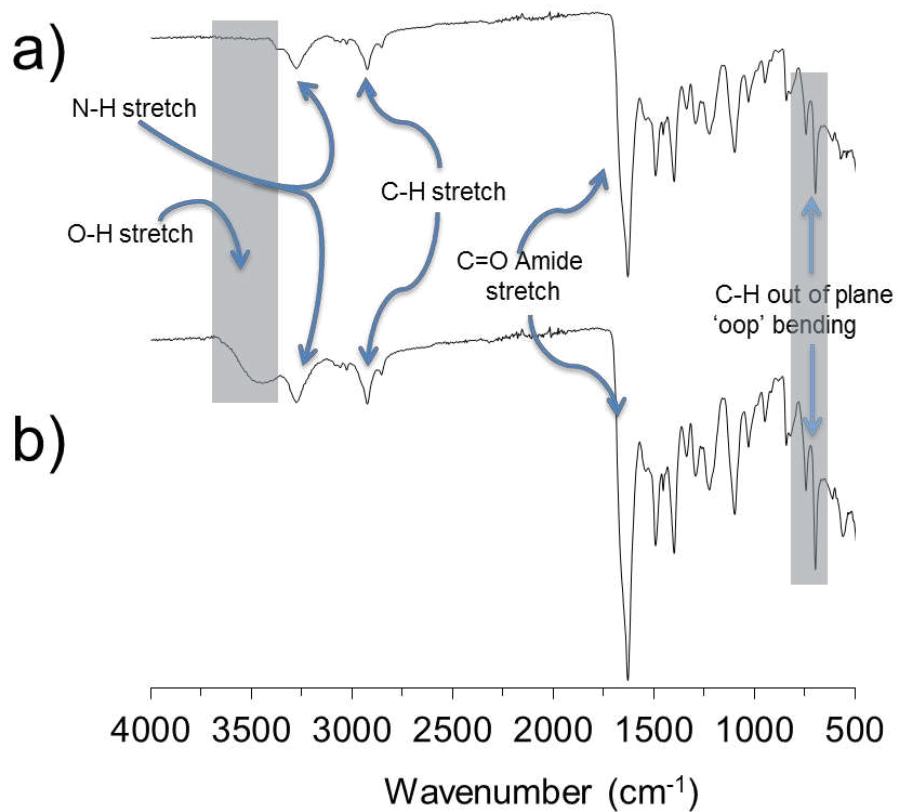
Figure S10. FTIR spectra of Glu-poly(Sar)-*b*-poly(Phe) before (a) and after (b) cleaving off the acetyl protecting groups from the terminal sugar moieties. The emergence of the broad OH stretch (*ca* 3420 cm^{-1}) on the FTIR spectrum of the deprotected polymer (b) confirmed the removal of the acetyl groups.

Dynamic Light Scattering

Table S5. DLS Analysis of the nanoparticles produced.

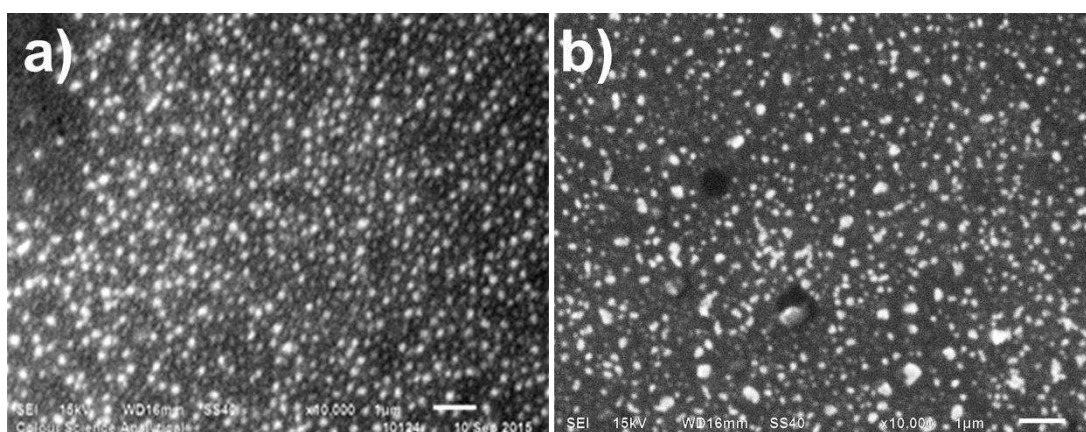| Polymer	Particle Size (nm)
Glu-poly(Sar)-*b*-poly(PheLA)	59.6 ±12
Glu-poly(Sar)-*b*-poly(Phe)	66.8 ±10

Figure S11. SEM microphotographs of nanoparticles formed from the synthesis of biodegradable block copolymers from Glu-poly(Sar)-*b*-poly(PheLA) (a) and Glu-poly(Sar)-*b*-poly(Phe) (b).
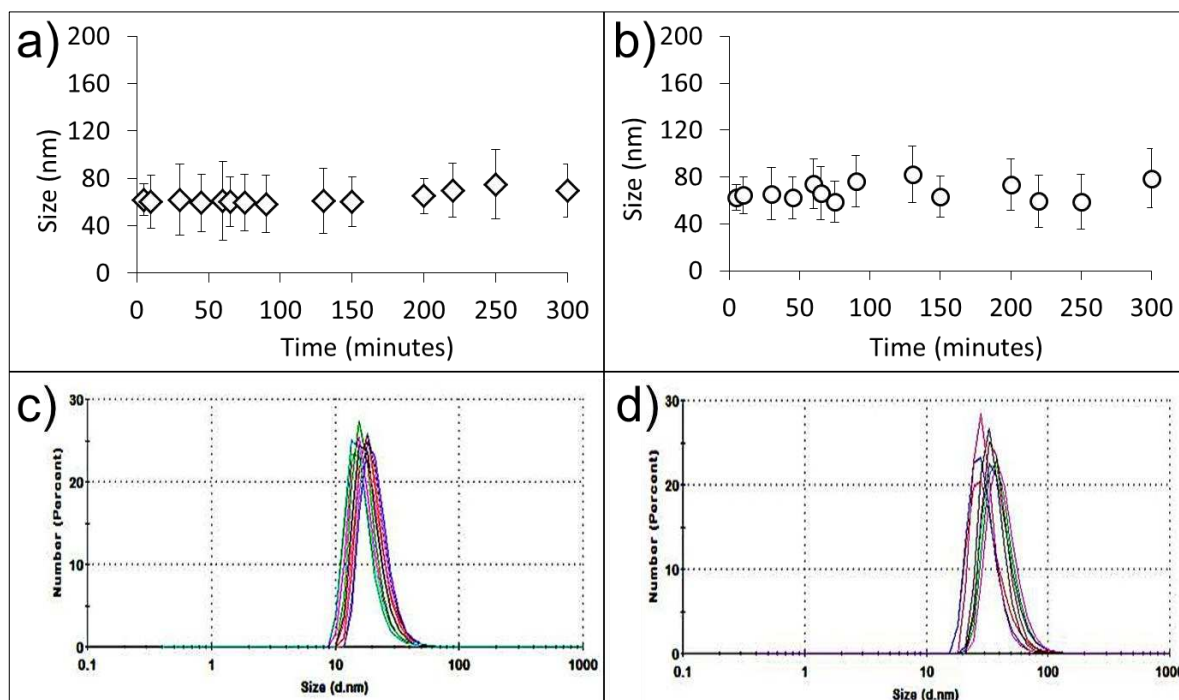
Figure S12. Stability of Glu-poly(Sar)-*b*-poly(Phe) nanoparticles (a) and Glu-poly(Sar)-*b*-poly(PheLA) nanoparticles (b) monitored continuously for 300 minutes. Both sets of nanoparticles were stored and re-analysed after 5 days and after 25 days. In both instances the particle size was found to have remained relatively unchanged. Error bars represent the standard deviation for DLS measurements done in triplicate. An overlay of the DLS traces confirms the close fit of the particle size (stability) at the various time intervals studied for Glu-poly(Sar)-*b*-poly(Phe) nanoparticles (c) and Glu-poly(Sar)-*b*-poly(PheLA) nanoparticles (d).

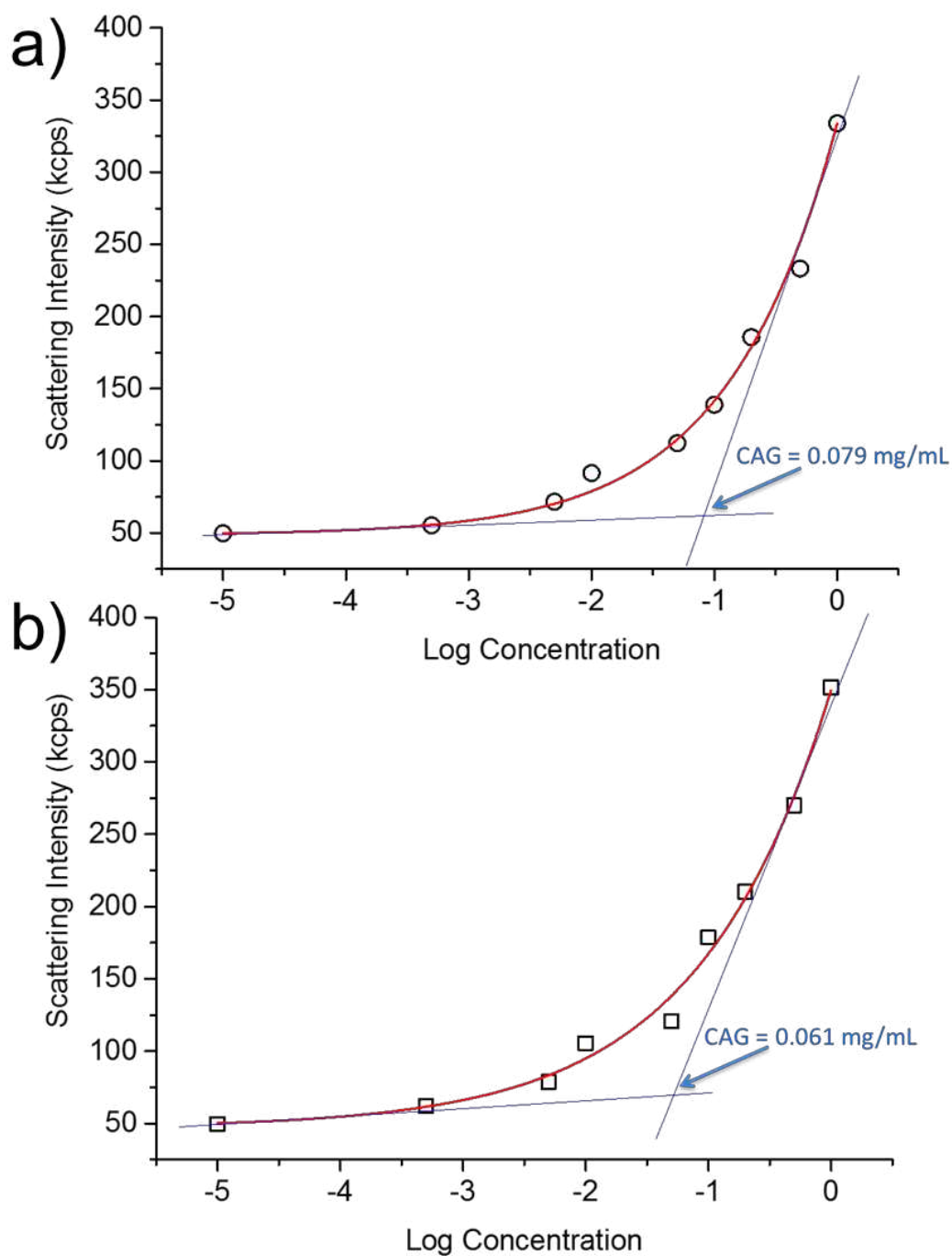# Critical Aggregation Concentration (CAG)

Figure S13. Determination of the critical aggregation concentration (CAG) of Glu-poly(Sar)-*b*-poly(Phe) (a) and Glu-poly(Sar)-*b*-poly(PheLA) (b) using the Malvern Instruments' method for determination of CAG using dynamic light scattering [3-5].
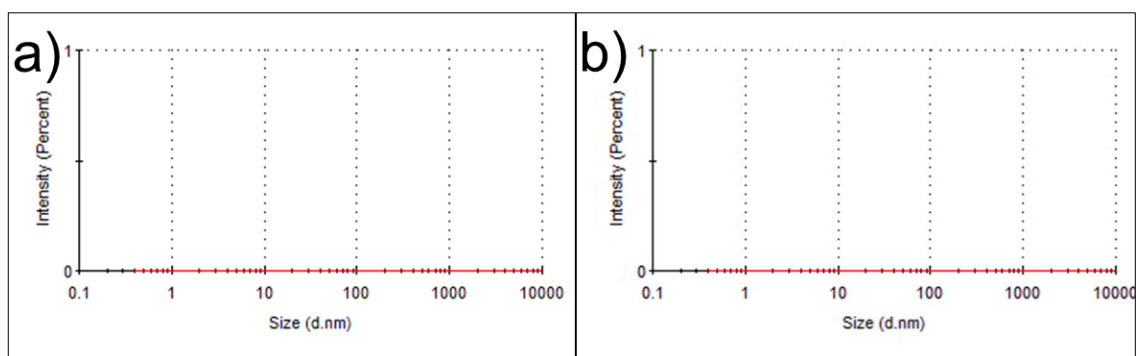
Interaction of Nanoparticles with Con A

Figure S14. DLS result obtained from aqueous solutions of RCA$_{120}$ lectin (a) and CON A lectin confirming absence of aggregates before lectin binding studies on nanoparticles.
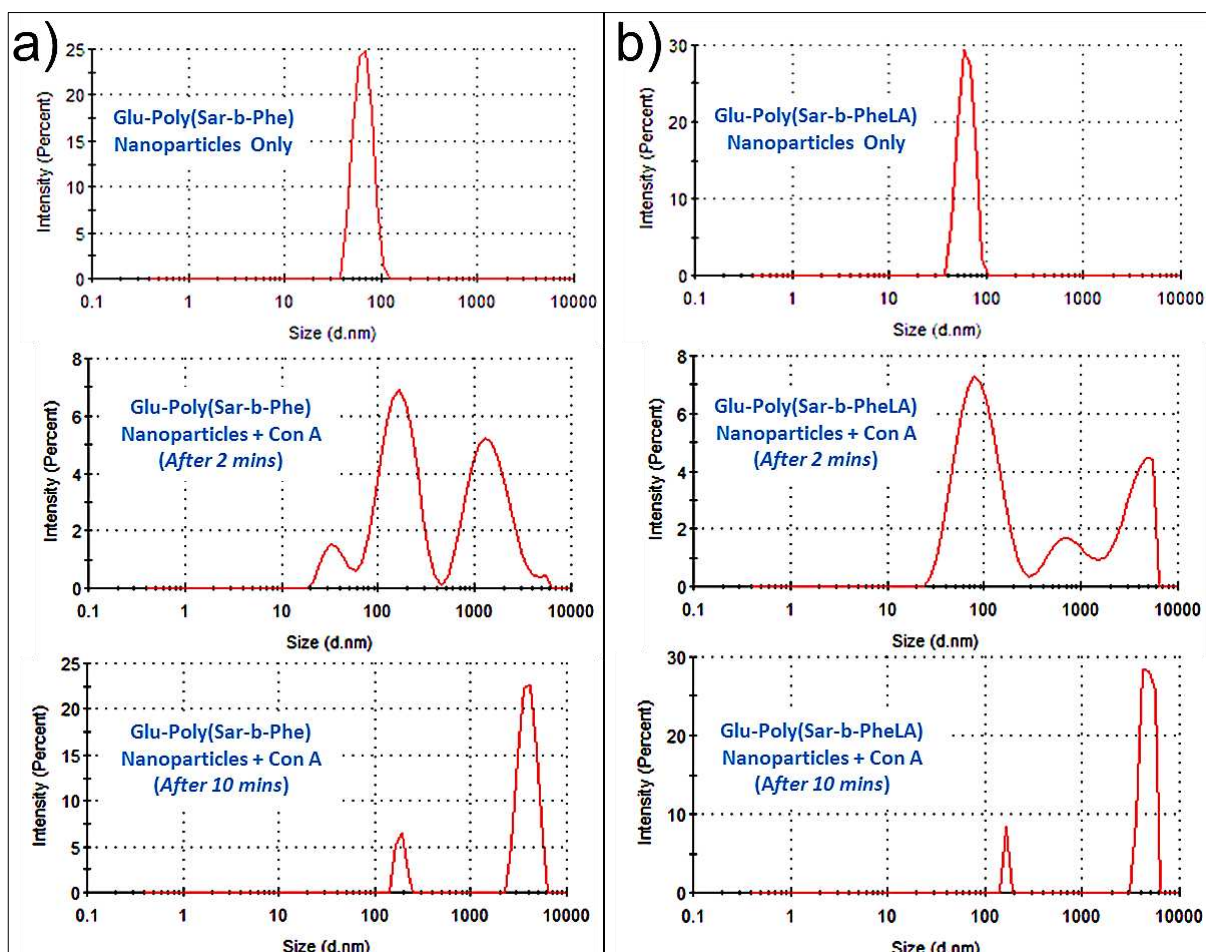

Figure S15. DLS traces obtained at different time intervals from the agglutination studies of Glu-poly(Sar)-*b*-poly(Phe) nanoparticles (a) and Glu-poly(Sar)-*b*-poly(PheLA) nanoparticles (b) with CON A, respectively, showing clearly the gradual complexation into large aggregates.
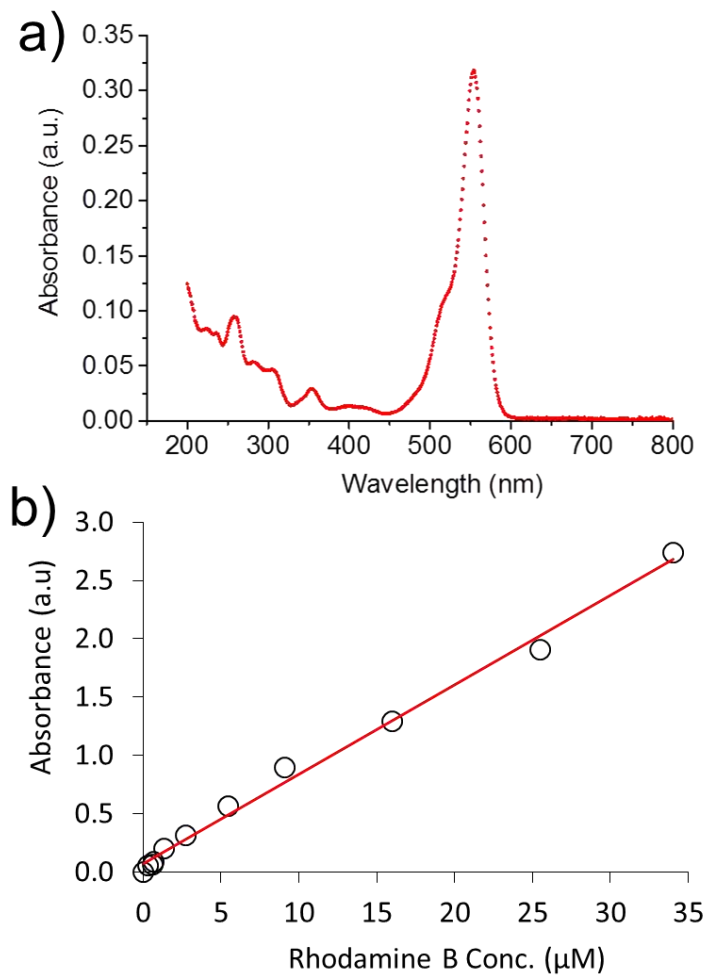
Degradation of Nanoparticles/Payload Release

Figure S16. Absorption spectrum of rhodamine B showing the λ_{max} at 554 nm (a) and the calibration linear graph used for computing the release of rhodamine B from Glu-poly(Sar)-*b*-poly(Phe) and Glu-poly(Sar)-*b*-poly(PheLA) nanoparticles, at λ_{max} (b).

Fitting Release Data into Korsmeyer-Peppas Model

$$\frac{M_t}{M_\infty} = kt^n$$

$$\log\ (\text{release}\ \%) = \log \left[\frac{M_t}{M_\infty}\right] = n \log t + \log k$$

Whereby, the slope (*n*) is the release exponent at time t;

- $n \leq 0.43$; Fickian diffusion

- $0.43 < n < 0.85$; non-Fickian (anomalous)

- *n* > 0.85; Case II transport   [6, 7]
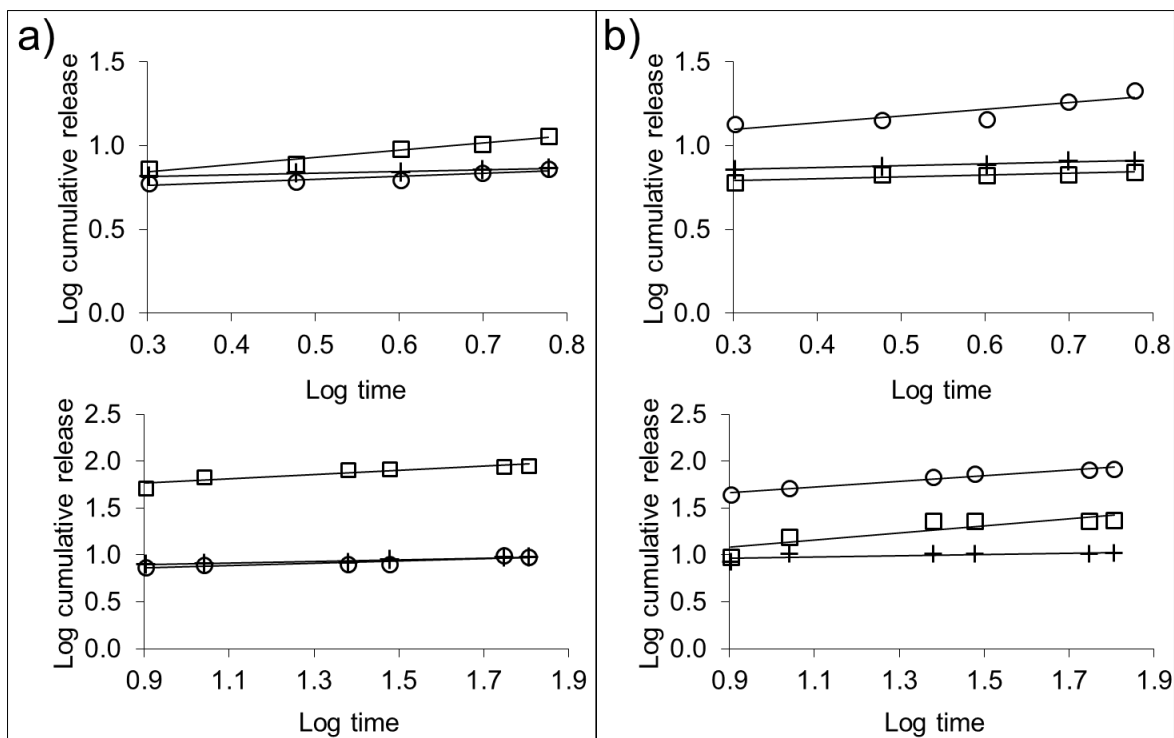
Enzyme-mediated release

Figure S17. Korsmeyer-Peppas model plots for the release of molecular cargo from Glu-poly(Sar)-*b*-poly(Phe) nanoparticles (a) and Glu-poly(Sar)-*b*-poly(PheLA) nanoparticles (b) incubated in PBS (pH 7.4) only (+), PBS (pH 7.4) plus Chymotrypsin (□), PBS (pH 7.4) plus Lipase (○), *(top: 0-8 hours, bottom: 9-65 hours)* respectively.

Table S6. The release exponents (*n*) obtained after fitting enzymatic degradation/release data into the Korsmeyer–Peppas (KP) model. The release exponent (*n*) ≤ 0.45 in all instances suggesting that the release of encapsulated cargo from the particles follows Fickian diffusion

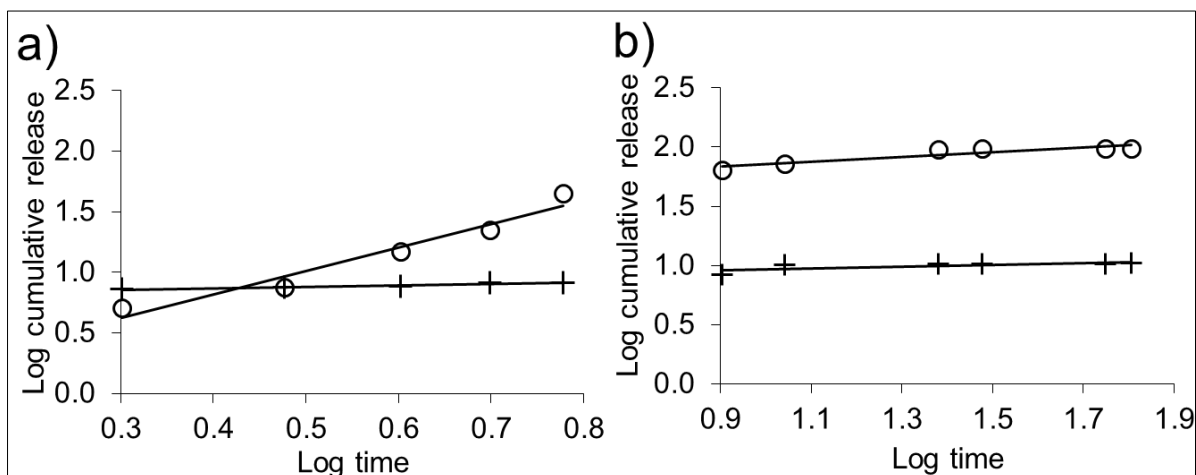|	0 - 8 hours	9 - 65 hours
	n	*n*
Glu-Poly(Sar)-*b*-Poly(Phe) in PBS only (pH 7.4)	0.10	0.09
Glu-Poly(Sar)-*b*-Poly(Phe) + Chymotrypsin (pH 7.4)	0.40	0.23
Glu-Poly(Sar)-*b*-Poly(Phe) + Lipase (pH 7.4)	0.18	0.13
Glu-Poly(Sar)-*b*-Poly(PheLA) in PBS only (pH 7.4)	0.11	0.07
Glu-Poly(Sar)-*b*-Poly(PheLA) + Chymotrypsin (pH 7.4)	0.11	0.37
Glu-Poly(Sar)-*b*-Poly(PheLA) + Lipase (pH 7.4)	0.43	0.30

Acidic pH-mediated release

Figure S18. Korsmeyer-Peppas model plots for the release of molecular cargo from Glu-poly(Sar)-*b*-poly(PheLA) nanoparticles (*0-8 hours (a) and 9-65 hours (b)*) incubated in PBS (pH 7.4, 37°C) (+) and acetate buffer (pH 5.4, 37°C) (○).

Table S7. The release exponents (n) obtained after fitting pH-mediated degradation/release data into the Korsmeyer–Peppas (KP) model.

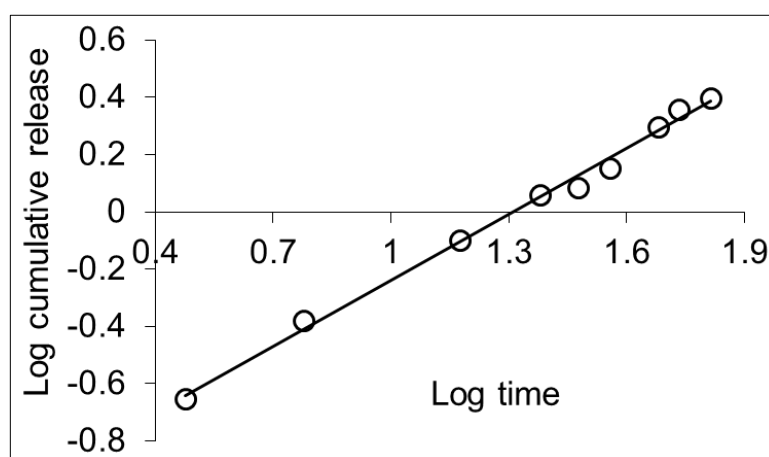|		Glu-poly(Sar)-*b*-poly(PheLA) in PBS (pH 7.4, 37°C)	Glu-poly(Sar)-*b*-poly(PheLA) in acetate buffer (pH 5.4, 37°C)
n	0 - 8 hrs	0.11	1.94
	9 - 65 hrs	0.07	0.20

Figure S19. Korsmeyer-Peppas model plots for the release of molecular cargo from Glu-poly(Sar)-*b*-poly(Phe) nanoparticles incubated in PBS (pH 7.4, 37°C) (+) and in acetate buffer (pH 5.4, 37°C) (○).

Table S8. The release exponent (n) obtained after fitting data from the pH-mediated swelling of Glu-poly(Sar)-b-poly(Phe) nanoparticles into the Korsmeyer–Peppas (KP) model.

	Glu-poly(Sar)-*b*-poly(Phe) nanoparticles in acetate buffer (pH 5.4, 37°C)
n (0 - 65 hrs)	0.77

References

1. X. Xu, G. Shan and P. Pan, *RSC Advances,* 2015, **5**, 50118-50125.

2. C. Cheng, X. Zhang, Y. Wang, L. Sun and C. Li, *New J. of Chem.*, 2012, **36**, 1413-1421.

3. R.B. Dorshow, C.A. Bunton and D.F. Nicoli, *The J. of Phys. Chem.*, 1983, **87**, 1409-1416.

4. Ö. Topel, B.A. Çakır, L. Budama and N. Hoda, *J. of Molecul. Liquids*, 2013, **177**, 40-43.

5. *Surfactant micelle characterization using dynamic light scattering*. http://quimica.udea.edu.co/~coloides/Anexo1.pdf. [Online Manufacturer database].

7. P. Costa and J.M. Sousa Lobo, *Europ. J. of Pharm. Sci.*, 2001, **13**, 123-133.

8. R. Huang, W. Qi, L. Feng, R. Su and Z. He, *Soft Matter*, 2011, **7**, 6222-6230.